Jurnal Kejuruteraan 13 (2001) 87-97

Structural Perturbations in Proton-Randomized Single Point Charge Simulated Ice

Ronald M. Pratt

ABSTRAK

Molecular dynamics, along with Monte Carlo methods, continue to be powerful tools to probe molecular behavior. In this study, we used a simulation cell consisting of 896 water molecules in an ice-1h configuration to compare structural properties of proton-randomized simulated ice using the Single Point Charge (SPC) potential model. A subtle, yet significant crystal defect is found in proton-randomized ice which involves two of the three mutually perpendicular dipole angle distributions. This deformity does not influence macroscopic behavior of the subtance, but it does indicate a departure in arrangement from the known structure of water. It is therefore recommended that an ordered ice structure first be set up, and then random perturnations made to achieve a proton disordered structure.

Key word: Molecular dynamics, SPC, Quaternions, Water Simulation, Ice, Dipole Angles

INTRODUCTION

With the development of high speed computers, molecular simulation is an effective method of carrying out experiment at a molecular level. In fact, computer simulation of atoms and molecules provides the experimental data by which molecular theories and models may be tested (Lee 1988). The concept of molecular simulation traces back to the time of Laplace's discourse on determinism which shaped not only science, but 19th century theology and philosophy as well (Laplace 1814):

> Given for one instant and intelligence which could comprehend forces by which nature is animated and the respective situation of the beings who compose it - an intelligence sufficiently vast to submit these data to analysis - it would embrace in the same formula the movements of the greatest bodies of the universe and those of the lightest atoms; for it, nothing would be uncertain and the future, as the past, would be present to its eyes.

Although later developments in physics have precluded the concept of a deterministic world, this deterministic view is still a reasonable approximation for probing the behavior of molecules and other large bodies (Haile 1992). Using the computer as Laplace's "suffficiently vast intelligence", molecular simulations roughly falls into two categories, molecular dynamics, and Monte Carlo. Molecular dynamics (Alder et al. 1959) sets up and numerically solves the equations of motion which govern the movement of a few hundred to a few thousand particles. System properties are then

average over time. Monte Carlo (Metropolis et al. 1953), on the other hand, avoids the concept of time altogether, and relies on a Markov chain of random perturbations to a similar sized system of particles. System properties calculated from the Monte Carlo method are ensemble averages. According to the Ergodic hypothesis (Haile 1992) both averaging methods are equally valid, and in the limit of infinite time and infinite number of system configurations, will yield exact results.

In this paper we use molecular dynamics to observe the molecular behavior of water and ice 1h (hexagonal, antiferromagnitic). In molecular dynamics, molecular configurations are normally represented using one of two methods: quaternions or constrant algorithms. Using quaternions (a mathematically friendly [Goldstein (1980) version of Euler angles] allows for rotational motion to be calculated by explicit integration of the Euler equations of motion (Evans 1977). In other words, equations are set up to represent both translational and rotational motion. When using constraint algorithms, only the translational equations of motion are integrated, but in such a way as to constrain bond lengths and bond angles to prescribed values (Ryckaert et al. 1977). The quaternion method is used in this study. When using quaternions, there are two equivalent methods of representing a water molecule's spatial configuration at any time, t:

1. the x, y, and z atomic positions af the oxygen and both hydrogen molecules (nine numbers).
2. the x, y, and z center of mass positions and four quaternion values (seven numbers).

Since, in fact, any three quaternion values are sufficient to determine the fourth (the squares sum to unity), only six numbers are needed to fully specify the position and orientation of a water molecule.

X-ray (Narten et al. 1971) and neutron (Thiessen et al. 1982) scattering experiments have been exhaustively performed on ice and liquid water and indicate that naturally occuring ice 1h contains a host of defects and irregularities. These deformities involve the oxygen as well as hydrogen atoms. This has encouraged simulators to employ randomized hydrogen positions in setting up ice crystal lattices.

SETUP AND RPOSEDURE

The FORTRAN simulation program used for this study incorporates the Single Point Charge (SPC) intermolecular potential model (Jorgenson et al. 1983). This is a rigid, three-site model, where the potential between any two water molecules may be calculated:

$$u(r_{i,j}) = \frac{A}{r_{0-0}^{12}} - \frac{A}{r_{0-0}^{6}} + \sum_{i=1}^{3}\sum_{j=1}^{3}\frac{q_i q_j e^2}{r_{i,j}} \qquad \text{(Eq. 1)}$$

where A = 629,400 Kcal-Å^{12}/mol and C = 625.5 Kcal Å^6/mol. The partial charge are q_o = –0.82 and q_H = +0.41. Indices i and j run over atomic sites of each of the two molecules. Equation 1 represents a single Lennard-Jones type interaction between the two oxygen atoms, and a total of nine Coulombic interactions between all the atoms. A system consisting of 896 molecules

was set up forming a nearly cubic parallelepiped with dimensions of 31.1 Å x 31.4 Å X 29.3 Å. The system was run at a constant temperature and density of 190K and 1.0 g/cm^3, respectively. The Beeman algorithm (Beeman 1976) was used to integrate the second-order rotational and translational equations of motion (Rapaport 1988) with a time step of 1.08 femptoseconds (10^{-15} s). Ewald sums were not used for these large systems, and a cutoff of 10 Å was employed. Standart periodic boundary conditions and the minimum image convention (Haile 1992) were used.

Two ice system were set up, one with assigned hydrogen position and one with randomized hydrogen positions. The former was set up providing maximum hydrogen bonding and minimum system dipole and configuration energy. The unit cell (containing eight water molecules) was replicated 112 times to form the nearly cubic simulation cell described above consisting of 896 water molecules. Tables 1 and 2 show the mutually aquivalent representations of the perfect Ice 1h unit cell. The SPC potential model assumes a tetrahedral structure, therefore bond angles of the water molecules have been changed to 109.47° from 104.5°.

The four quaternion values were found from Cartesian coordinates by solving the nine non-linear equations which result (Allan et al. 1990) using a simple multidimensional search. This hard to be done just once for each of the eight molecules in the unit cell. Since the simulation cell contained no hot sport or regions of local high temperature, equilibration was rapid. Initially the system was allowed to run at about 3K for about 500 time steps. During this time, the behavior of the system was static, and we next ramped the temperature up to 190K by scaling translational and rotational velocities. This was done rapidly, in about 1000 steps and already there was

TABLE 1. Cartesian coordinates (in Å) for ice 1h unit cell (8 water molecules)

	1	2	3	4	5	6	7	8
x_O	0.9427	2.2391	4.8318	6.1282	0.9427	2.2391	4.8318	6.1282
y_O	0.8165	3.0619	3.0619	0.8165	0.8165	3.0619	3.0619	0.8165
z_O	1.9167	1.0000	1.9167	1.0000	4.6667	5.5833	4.6667	5.5833
x_{H1}	0.9427	1.7677	3.8890	5.6568	1.4141	1.7677	4.8318	5.6568
y_{H1}	0.8165	3.8784	3.0619	0.0000	0.0000	2.2454	3.0619	1.6330
z_{H1}	2.9167	1.3333	1.5833	1.3333	5.0000	5.2500	3.6667	5.2500
x_{H2}	1.4141	2.2391	5.3032	7.0710	0.0000	3.1819	5.3032	6.1282
y_{H2}	1.6330	3.0619	2.2454	0.8165	0.8165	3.0619	3.8784	0.8165
z_{H2}	1.5833	0.0000	1.5833	1.3333	5.0000	5.2500	5.0000	6.5833

TABLE 2. Center of mass positions (in Å) and quaternions for ice 1h unit cell

	1	2	3	4	5	6	7	8
x_{CM}	0.9689	2.2129	4.8056	6.1544	0.9165	2.2653	4.8580	6.1020
y_{CM}	0.8619	3.1072	3.0165	0.7711	0.7711	3.0165	3.1072	0.8619
z_{CM}	1.9537	0.9630	1.8796	1.0370	4.7037	5.5463	4.6296	5.6204
q_1	-0.0300	0.0300	0.0800	-0.0800	-0.9200	-0.0800	-0.0300	0.0300
q_2	0.6000	0.6000	0.2500	0.2500	0.2900	-0.2500	-0.6000	-0.6000
q_3	0.3800	-0.3800	-0.9200	0.9200	0.0800	-0.9200	-0.3800	0.3800
q_3	0.7034	0.7033	0.2910	0.2910	0.2510	0.2910	0.7033	0.7033

equipartitioning of translational and rotational kinetic energy. We now allowed a generous time for system equilibration, about 250,000 time steps or more than 250 picosecond. Data collection runs of 10,000 time steps were then made and successive runs showed no statiscally significant change whatsover in system behavior.

The proton-randomized system was set up similarly except that the quaternions were not calculated from known atomic positions, but assigned randomly. The only constraint was that the sum of the four quaternion values sum to unity (Goldstein 1980). The initial behavior of this system was radically different that the proton-ordered system above. Initially, the system was run at 3K, but the unnatural moleculer orietations caused the molecules to spin in place at very high velocities. Startup results for both the randomized and assigned system are shown in Figure 1. We see than within the first 10 timesteps the rotational kinetic energy of the randomized system shot up to nearly 7000 kcal/mol, or a temperature of over 1000K. Notice that the rotational and translational energies for the proton-assigned system are both essentially zero in Figure 1 and cannot be seen.

A problem arose since this rotational kinetic energy immediately began to be diverted off to translational motion (equipartitioning of rotational and translational energy was achieve in about 150 time steps as we seen in Figure 1). When the translational kinetic energy exceeds approximately 1000 cal/mol, the lattice begins suffers damage within just a few time steps; i.e., the water molecules have enough translational energy to break out of their lattice positions. This effect is not desired. Therefore, the run was cancelled and the lattice reinitialized.

We now modified the program to reset translational velocities, accelerations, and forced to zero at each timestep for each of the 896 water molecules. Now, the rotational energy could not be transferred to translational energy since the translational temperature was fixed at absolute zero. Restarting the simulation under these conditions, the rotational velocities again shot up to extremely high values, as nature worked to relieve stresses in the system. After 2000 timesteps of running with extremely high rotational temperatures and zero K translational temperatures, the rotational velocities

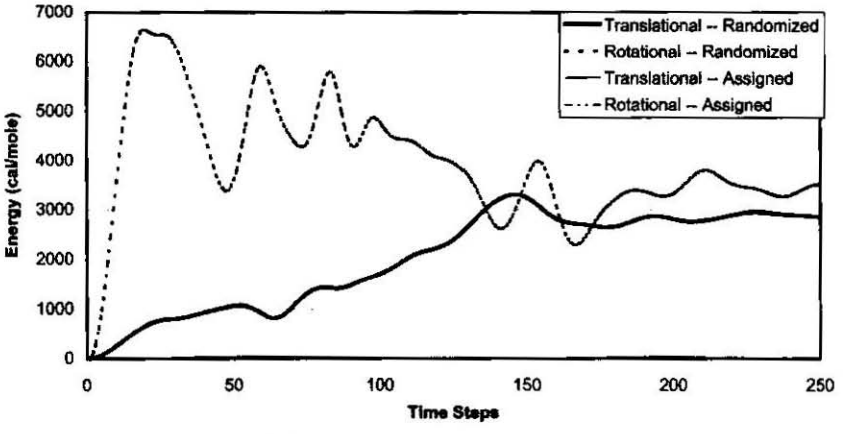

FIGURE 1. Startup behaviour for proton ordered and disordered ice

were gradually, over 2000 additional time steps, rescaled back to 3K. The system was allowed to run at this low temperature for a few hundred time steps, and then the constraints on the translational positions were removed. The temperature was slowly ramped up to 190K by rescaling translational and rotational velocities over about 2000 more timesteps. This achieved relaxation or annealing of the ice crystal without destroying or perturbing the original lattice structure. The system was then given over one nanosecond (>1,000,000 timesteps) to equilibrate at 190K with no artificial constraints. Again, data collecting runs were made following equilibration consisting of 10,000 time steps. From this setup method, we see that the proton-disordered system is equivalent to performing simulated annealing on the rotational velocities.

DISCUSSION

Various physical properties were calculated for both systems. In addition, properties were calculated for an analogous liquid water system at 190K (although the melting point of SPC ice is 240K, SPC ice will not crystallize at temperatures below the melting point, rather it forms a viscous, glassy substance). We first look at the radial distribution functions, g (r), which indicate the influence of any given molecule on the nearby bulk/local density ratio as a function of distance. At large distanced (approximately 8 Å) molecules are sufficiently screened from each other so as to have no mutual effect and the g(r) value approaches unity. These g(r) curves were measured directly by accumulating histograms throughout the lenght of the simulation run. Figure 2-4 show the Oxygen-Oxygen, Oxygen-Hydrogen, and Hydrogen-Hydrogen radial distribution functions respectively. Very little difference is observed between the proton-randomized and proton-assigned ice structures for $g_{oo}(r)$ $g_{oh}(r)$. Liquid water shows significantly reduced peaks in all three curves which is expected for an isotropic fluid. Some discrepancy, though not particularly remarkable, however, is observed in $g_{HH}(r)$ in Figure 4, and is due to long term failure of the disordered system to equilibrate into the ordered system configuration.

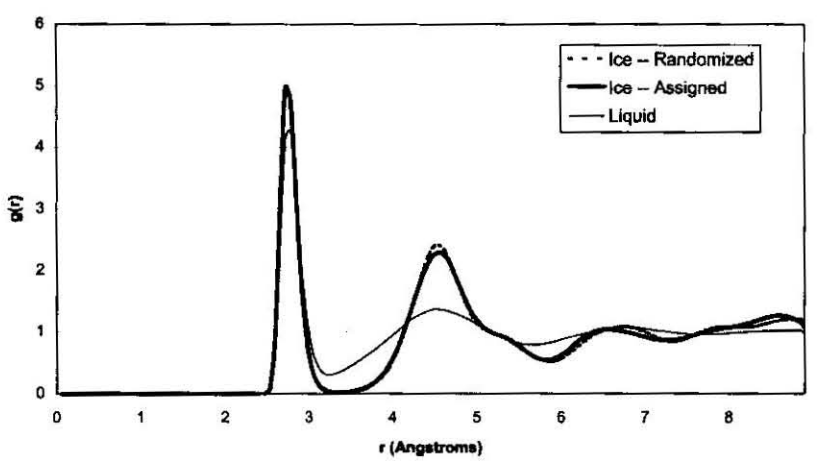

FIGURE 2. Oxygen - Oxygen radial distribution functions

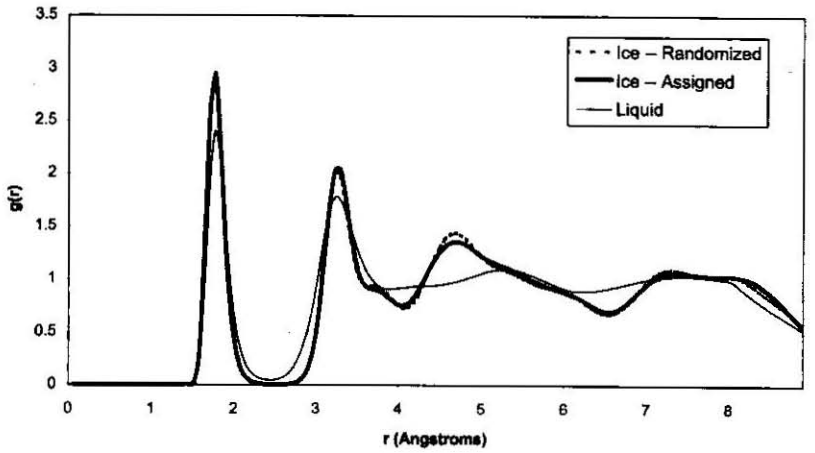

FIGURE 3. Oxygen - Hydrogen radial distribution functions

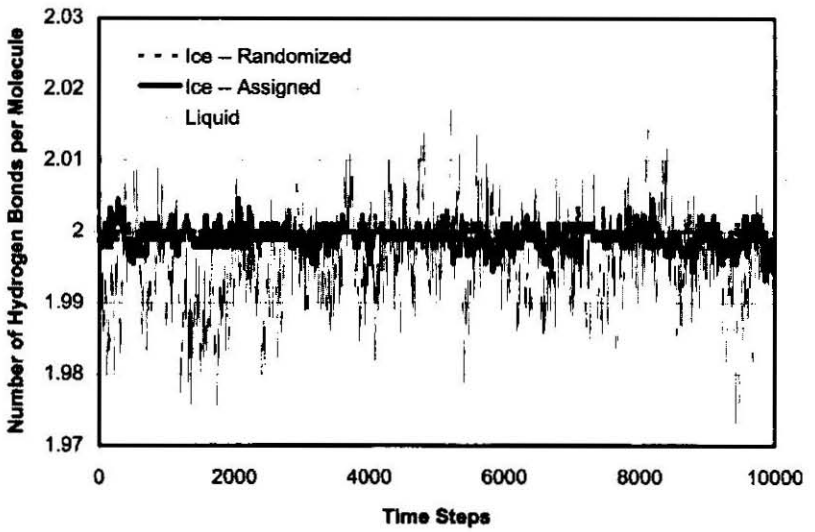

FIGURE 4. Hydrogen - Hydrogen radial distribution functions

We next consider the hydrogen bonding features of liquid water and the two ice structures. Figure 5 shows the number of hydrogen bonds per molecule, which should be exactly two for perfect hydrogen bonding (a perfect crystal at zero K). There is no difference in the average number of hydrogen bonds for both ice systems. This shows that the annealing process which occured for the randomized system achieved full hydrogen bonding. We also observed that melting ice into liquid water destroys very few of the hydrogen bonds. Figure 6 shows the average hydrogen bend length, averaged over all bonds over the length of the simulation. The two ice curves are coincidental, showing a narrow distribution about the hydrogen bond length for water, 1.74 Å. The corresponding curve for liquid water shows a slightly widened distribution and a slightly lengthened hydrogen bond length. In Figure 7 we see to what extent the hydrogen bond (O-H-O) angles deviate from linearity. For a perfect crystal, the bonds should be perfectly linear.

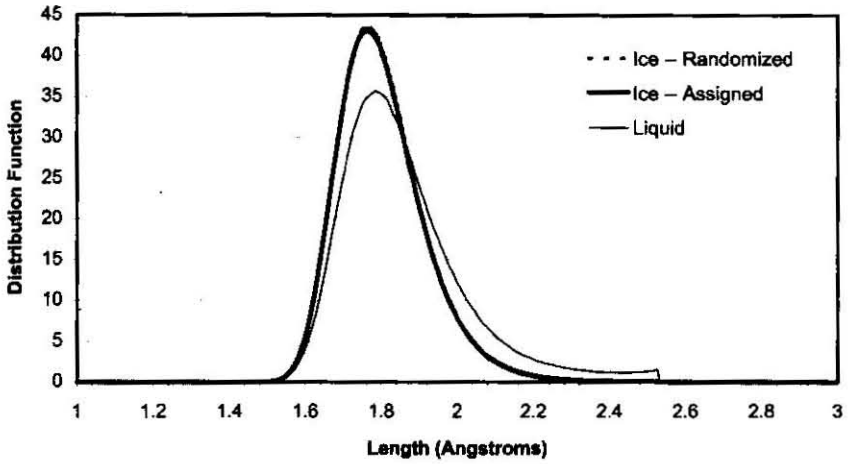

FIGURE 5. Number of hydrogen bonds per water molecule

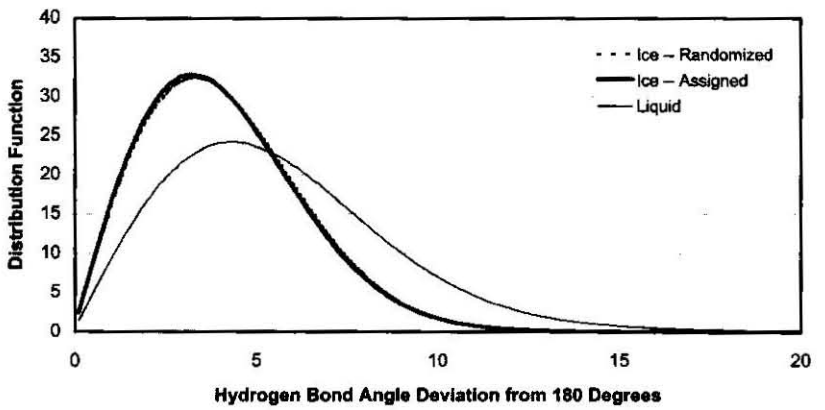

FIGURE 6. Hydrogen bond length distribution

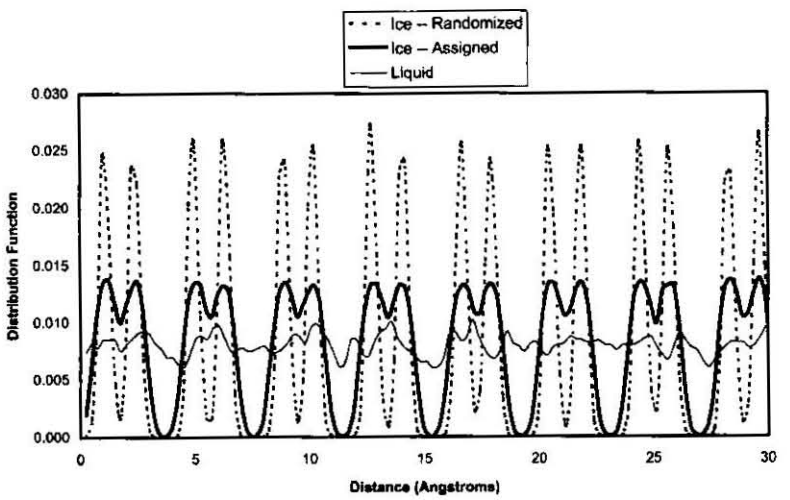

FIGURE 7. Hydrogen bond angle distribution

Again, for the two ice systems, the curves are coincidental with an average hydrogen bond angle 180°±4°. For liquid water, the devation is slightly increased to ±4.5° and the distribution curve is slightly widened. We observed absolutely no difference in hydrogen bonding features of the two ice systems.

Figure 8-10 show oxygen density profiles for the two ice and the water systems. These profiles were obtained by dividing the system into a number of thin, parallel slices about 2 Å thick and counting the number of oxygen molecules in each slab. These thin slabs were made in each of three mutually orthogonal directions yielding three difference curves. In Figure 8 and 9 we observed double peaks, in Figure 10, we do not. (This is obvious if we construct a sufficiently large ball-and-stick ice model). Liquid water, which has no crystal structure, shows no peaks and troughs, only small and

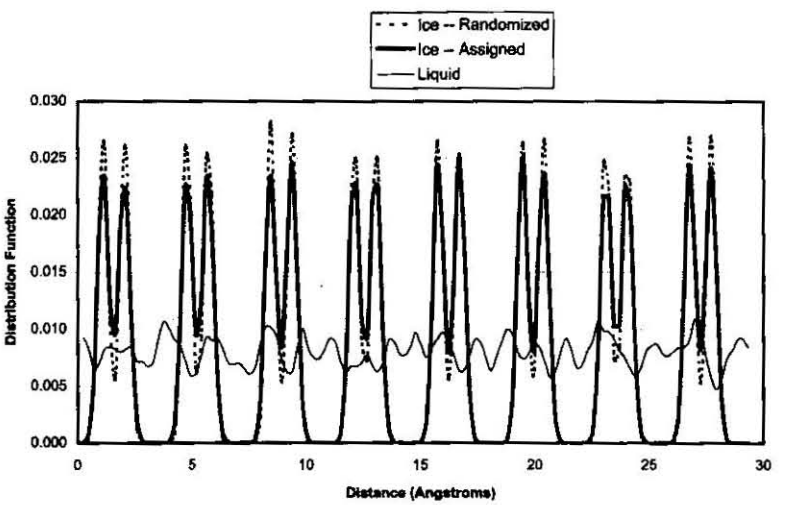

FIGURE 8. Oxygen desity profile 1

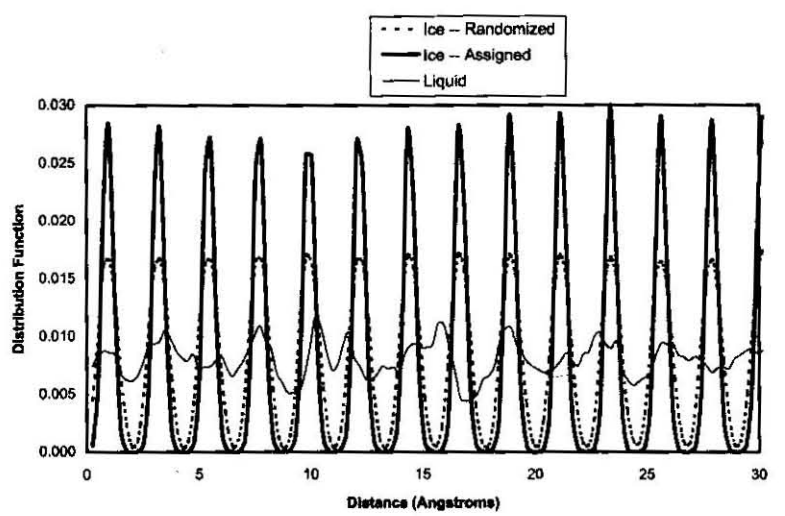

FIGURE 9. Oxygen density profile 2

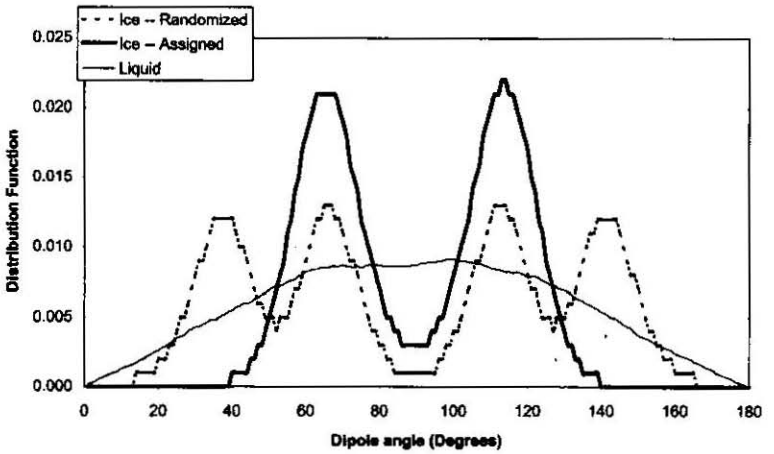

FIGURE 10. Oxygen density profile 3

uniform random fluctuations. In each of these three figures, we observed a consederable difference in the behavior of proton-ordered and proton-disordered ice. In Figure 8 and 9, the proton ordered system has lower peaks, in Figure 10, the proton ordered system has higher peaks. We observed that the difference placement of the hydrogen atoms influences the average position of the oxygen molecules in the lattice.

In Figure 11-12 we plot the dipole angle distribution, which is the distribution of angles made by the dipole of each water molecule and each of the three orthogonal axes. (In all three systems after equilibration, the net system dipole fluctuated near zero). The dipole angle is calculated from the dipole vector, D_v:

$$D_v = (q_0 x_0 + q_{H1} x_{H1} + q_{H2} x_{H2})\hat{i} + (q_0 y_0 + q_{H1} y_{H1} + q_{H2} y_{H1})\hat{j} + (q_0 z_0 + q_{H1} z_{H1} + q_{H2} z_{H2})\hat{k} \quad \text{(Eq. 2)}$$

and then calculating the angle between D_v and one of the three orthogonal axes, A:

$$\theta = \arccos\left[\frac{D_v \cdot A}{|D_v||A|}\right] \quad \text{(Eq. 3)}$$

The angle, θ, can vary from 0° to 180°. Liquid water, being isotropic, should have a sinusoidal dipole angle distribution with a peak at 90° and tapering to zero at each end. (Karim et al. 1988) and we observe this in all three figures. The three sets for a perfect ice 1h crystal at zero K should have spikes or delta-type functions at (65° and 114°), (44° and 134°), and (54° and 125°) (Pratt 1994). For a real crystal at finite temperature, these spikes will be replaced by normal or Gaussian distributions about these values. This is seen in Figures 11-12 for the proton ordered systems. However, Figures 11 and 12 show completely different fistributions for the disordered system. This is where we observe the most pronounced difference between the two ice systems. We observe that the proton disordered system in unable to anneal itself or equilibrate into ordered system behavior.

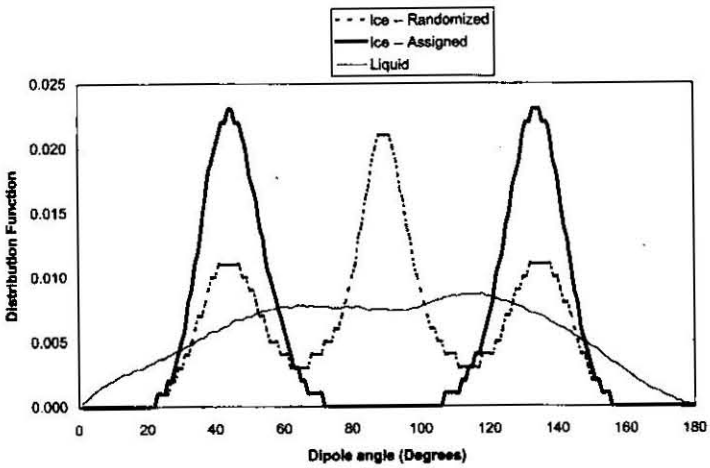

FIGURE 11. Dipole angle distribution 1

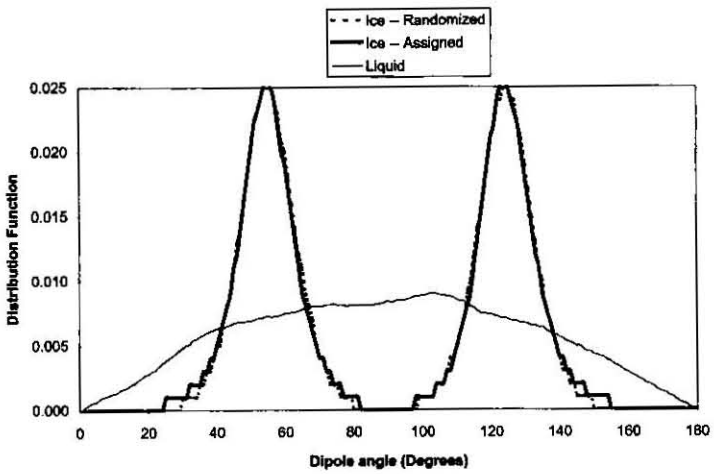

FIGURE 12. Dipole angle distribution 2

CONCLUSIONS

Which of the two ice systems most closely resembles actual ice? Probably the proton disordered system, since we know that physical ice contains many crystal defects. However, it is not clear that the defects manifested by randomized (or annealed) proton locations reflect the defects found in physical ice. Unfortunately, experimental dipole angle distribution are not available for hexagonal ice and a direct comparison cannot be made. Such measurements have been made, however, for cubic ice (Dore 2000). We do know that an ice lattice with no defects will exhibit the behavior as observed in the proton-assigned system. From this study, then we conclude:

1. Proton disordered ice, even after extensive equilibration time, does not crystallize into a perfect lattice. There are permanent defect, most clearly revealed in the dipole angle distribution.

2. Some features of the randomized ice sample appear more liquid like than the non-randomized system, other features are more crystal-like.
3. Physical features of the hydrogen bonding, namely, number, length, and angle are not influenced by initial placement of the hydrogen atoms.
4. Hydrogen bonding features of liquid water are very similar to those of solid ice.

ACKNOWLEDGEMENTS

Gratitude is expressed to Prof. Kumar and Dr. Raymond Mountain for fruitul discussions and aid in setting up the ice lattices.

REFERENCES

Alder, B. J., & Wainwright, T.E. 1959. Studies in molecular dynamics. I. general method. *J. Chem. Phys.* 31: 459.

Allen, M. P., & Tildesley, D. J. 1987. *Computer Simulation of Liquids.* Oxford: Clarendon Press.

Dore, J. Personal Communication.

Evans, D. J. 1977. On the representation of orientation space. *Mol. Phys.* 34: 317.

Goldstein, H. 1980. *Classical Mechanics.* Reading: Addison-Wesley.

Haile, J. M. 1992. *Molecular Dynamics Simulation, Elementary Methods.* New York: Wiley Interscience.

Jorgensen, W. L., Chandrasekhar, J. & Madura, J. D. 1983. Comparison of simple potential functions for simulating liquid water. *J. Chem. Phys.* 79(2): 926.

Karim, O.A. & Haymet, A.D.J. 1988. The ice/water interface. *J. Chem. Phys.* 89 (11): 6889.

Laplace, P.S., 1814. Philosophical essay on probabilities. English tranlation by F. W. Presscott and F.L. Emory reprinted in *The Beginning of Modern Scince*, Walter J. Black Publisher, 1948, New York.

Lee, L.L. 1988. Molecular *Thermodynamics of Nonideal Fluids.* Boston: Butterworths.

Metropolis, N., Rosenbluth, A.W., Rosenbluth, M.N., Teller, A.H. & Teller, E. 1953. Equation of state calculations by fast computing machines. *J. Chem. Phys.* 21: 1087.

Narten, A. H. & Levy, H. A. 1971. Liquid water: moleculer correlation functions from X-tray diffraction, *J. Chem. Phys.* 55(5): 2263.

Pratt, R. M. 1994. Molecular Dynamics Simulation of Clathrate Hydrates, Hydrophobic Interactions, and Fractal Modeling of Clathrate Hydrate Systems. Doctora Thesis Colorado School of Mines, Department of Chemical Engineering and Petroleum Refining.

Rapaport, D.C., 1998. *The Art of Molecular Dynamics Simulation.* Cambridge: Cambridge University Press.

Ryckaert, J.P., Ciccotti, G., & Berendsen, J.J.C. 1977. Numerical integration of the Cartesian equations of motion of a system with constraints: molecular dynamics of n-alkanes. *J. Comput. Phys.* 23: 327.

Thiessen, W.E. & Narten, A.H. 1982. Nuetron diffraction study of light and heavy water mixtures at 25°C. *J. Chem. Phys.* 77(5): 2656.

Ronald M. Pratt
Lecturer,
Department of Chemical
and Process Engineering
Universiti Kebangsaan Malaysia
43600 UKM Bangi
Selangor D.E.
e-mail: rpratt@eng.ukm.my